Toughness Anisotropy in X70 and X80 Linepipe steels

M. S. Joo[a], D.-W. Suh[a], J.-H. Bae[b], H. K. D. H. Bhadeshia[a,c]

[a] *Graduate Institute of Ferrous Technology, POSTECH, Republic of Korea*

[b] *Technical Research Laboratories, POSCO, Republic of Korea*

[c] *Materials Science and Metallurgy, University of Cambridge, U.K*

Abstract

The anisotropy of mechanical properties in the context of steels used to fabricate large diameter pipes can be detrimental to the design and performance of the pipes. We examine here the anisotropy of strength and toughness, and with the help of detailed characterisation show that there is a complex interaction between the ability of the steel to delaminate on the rolling plane, and the crystallographic texture which promotes brittle fracture on the macroscopic fracture plane of Charpy specimens.

Keywords: linepipe steels, anisotropy, Charpy toughness, crystallographic texture, mechanism of anisotropy

1. Introduction

Large diameter pipelines are often made from plate which is wound into spirals to form the cylindrical shape, followed by welding. The original plate usually has anisotropic properties, which then are inherited in the pipe. Because of the spiral fabrication, the longitudinal direction of the plate is not parallel to that of the pipe. The lowest toughness direction in the plate is found at 45° to its rolling direction, which corresponds to the circumferential orientation of the pipe. Therefore, the toughness of the pipe will be minimum at the hoop orientation which also experiences the largest stress due to internal pressure [1–4].

Email address: dongwoo1@postech.ac.kr (D.-W. Suh)

The orientation dependence of toughness in hot–rolled steels is a well–researched area [5–24] and the cause is attributed to anisotropic inclusions or nonuniform distribution of inclusions, microstructural anisotropy and crystallographic texture. Such anisotropy limits the optimum design and exploitation of the steel.

In this context, some critical experiments on a specific X80 steel[1] have been reported that separate the roles of texture and other features that contribute to toughness anisotropy [26, 27]. It is the intention here to explore whether the conclusions reached are generic across different X70 and X80 linepipe steels.

2. Experimental method

The steels studied are listed in Table 1 along with the reference steel from previous work. The carbon content of the $X80$ steel is lower than that of $X80_{REF}$ to enhance low temperature toughness. In contrast, the $X70$ has a reduced manganese concentration to mitigate banding in the microstructure. The processing conditions are also listed in Table 1 and the final thickness of the steel was 18 mm.

Tensile specimens were prepared as illustrated in Fig. 1 and tested at ambient temperature, using a crosshead speed of 3.6 $\mathrm{mm\,min^{-1}}$ (strain rate $\approx 0.001\,\mathrm{s^{-1}}$). Full–sized Charpy specimens $10 \times 10 \times 55$ mm, each with a 2 mm-deep V–notch, were tested between ambient temperature to -100°C; details of the orientations are presented in Fig. 1c, which also contains the definitions of terminology. The Charpy samples were machined by removing 4 mm from each surface of the steel plates to achieve the 10 mm thickness.

Most of the observations of microstructure and crystallographic texture were conducted on four surfaces: the rolling plane, and on surfaces normal to the rolling plane but parallel to the expected planes of fracture of the three orientations of the Charpy specimens (Fig. 1). Micrographs were taken at random locations on these surfaces using optical and field emission scanning electron microscopy. The specimen preparation techniques have been described elsewhere, including those for transmission electron microscopy and

[1]The letter 'X' refers to pipe steel containing Cr, Cu, Mo, Ni, Si, Ti, V, Nb and Zr in any combination, whereas the digits specify the minimum yield strength in ksi [25]

electron back scattered diffraction [26].

3. Results and Discussion

3.1. Microstructure and Hardness

The microstructure of $X80_{REF}$ has previously been reported [26]; it is banded with coarse allotriomorphic ferrite and fine bainitic ferrite, together with pearlite, cementite, and the so-called MA constituent that contains a mixture of martensite and retained austenite. Full details are available in the original publication and a huge quantity of experimental observations have been archived on http://www.msm.cam.ac.uk/phase-trans/2012/X80.html

Figs. 2a,b show the microstructure of the $X80$ steel, with fewer precipitates than $X80_{REF}$ because of its lower carbon concentration, although a degree of banding is evident. Fig. 2c is an EBSD map showing the spread in crystallographic orientation; darker contrast indicates grains which are crystallographically homogeneous, i.e., with little internal misorientation due for example, to dislocation clusters. Allotriomorphic ferrite is associated with a low dislocation density and hence can be separated as the grey regions within which the misorientation is $< 1.5^\circ$ and where the microhardness was found to be 221 ± 4 HV. The remainder of the microstructure is bainitic ferrite with relatively larger dislocation density than grey regions and a greater hardness of 250 ± 4 HV. There is also evidence of MA phase in Fig. 2d, but unlike $X80_{REF}$, pearlite is absent, again consistent with the relatively low carbon concentration.

The essential features of $X70$ are similar to the $X80$, Figs. 3, with the exception that there is some evidence of pearlite in the MA regions and the hardnesses of the allotriomorphic ferrite and bainitic regions are slightly greater at 227 ± 5 and 256 ± 4, respectively. The quantity of allotriomorphic ferrite is also larger in the X70 steel. Table 2 lists the quantitative data determined using electron back-scattered diffraction in its image quality mode.

The grain size relevant to mechanical properties is not always that measured using optical microscopy [28]. Many adjacent, optically visible grains, may in fact be similarly oriented and hence have substantial crystallographic continuity across their boundaries. In such cases, it is the cluster of similarly oriented grains that define a size that correlates with the scale of cleavage

facets during brittle fracture. The definition of a crystallographic grain size requires an assumption of the misorientation that can be tolerated within the grain. Unfortunately, the specification of this misorientation can be arbitrary; for bainitic steel it has been assumed to be 15° [29] and 12° for thermomechanical controlled rolled steels [30]. Whether this is the correct choice remains to be proven. Therefore, the grain sizes calculated as a function of misorientation (2°, 15°) are listed in Table 3. They do not differ much between the steels studied, irrespective of the definition of the crystallographic grain size. The consequence of the choice is illustrated in Fig. 4, which also highlights the banded form of the microstructure.

Inclusions, such as complex oxides or alumina and calcium sulphide, were observed but mostly in spheroidal form and hence are judged not to influence the orientation dependence of Charpy toughness. These results are not reported here but are available for inspection [31].

3.2. Tensile and Charpy Properties

The tensile properties measured on samples machined parallel to the rolling plane (Fig. 1) are listed in Table 4. They reveal little variation as a function of test orientation, although all three alloys are strongest when tested normal to the rolling direction, consistent with reported observations on pipeline steel where the greater strength along the transverse direction was attributed to a strong presence of $\langle 110 \rangle$ directions parallel to the rolling direction, a crystallographic texture which according to model predictions maximises the strength parallel to the transverse direction [32]. The reason for this behaviour is that when $\langle 110 \rangle \parallel$ RD the $\{110\}$ planes which represent the prominent slip planes in ferrite tend to be parallel to the transverse direction, making slip relatively difficult. As seen later, this is precisely the kind of texture observed in the present studies.

When compared against the tensile strength data, the Charpy properties are found to be much more orientation dependent when tested in the temperature range corresponding to the ductile-brittle transition Fig. 5. It is noted that the extent of anisotropy is less than previously reported for $X80_{REF}$ [26]. The fracture surfaces of the broken Charpy specimens are shown in Fig. 6; they consistently show that delamination occurs for all the sample orientations when the test temperature falls in the ductile-brittle transition regime (-20 to -60°C for $X80$ and -60 to -80° for $X70$) which explains the

reduced anisotropy relative to $X80_{REF}$, Fig. 5,. The minimum in toughness seen at the D-D orientation for samples tested at -80°C in the X70 steel is clearly because of the lack of gross delamination when compared against the two adjacent orientations (Fig.. 5). Similarly, the smaller minimum observed at the D-D orientation for the X80 steel tested at -60°C is attributed to the relatively smaller delamination compared with the other orientations.

Delamination is associated with banding due to rolling. It remains to address why delamination is less pronounced for the D-D orientation. The plane on which the separation occurs is normal to the long direction of the notch. Therefore, for all the Charpy orientations, the delamination occurs on the rolling plane. In contrast, the fracture plane of the Charpy specimen (parallel to its cross-section) has its normal within the rolling plane. Cleavage fracture occurs easily if this macroscopic fracture plane has a high probability of encountering {100} ferrite planes on which cleavage normally occurs [33]. Such a scenario would lead to brittle behaviour at a stress which is not large enough to induce delamination.

To summarise, the Charpy energy recorded will be small when the stress required to cleave along the macroscopic fracture plane of the test sample is smaller than that required to produce delamination in the rolling plane. This reason may be associated with texture, and hence the experiments reported below.

3.2.1. Role of crystallographic texture

Experiments were done to assess any role that crystallographic texture may have on the observed anisotropy of mechanical properties. Fig. 7 shows the $\phi_2 = 45°$ sections of the ODF (orientation distribution function) of the bulk texture in all the steels. The textures of the two steels are similar. The pole figures are shown in Fig. 8, revealing a strong $\{112\}\langle 110\rangle$ and the rotated-cube texture $\{001\}\langle 110\rangle$ components. It is seen from Fig. 8 that the rotated-cube texture makes the diagonally oriented Charpy specimens particularly prone to brittle fracture with a strong alignment of the {100} planes parallel to the macroscopic fracture plane. This is consistent with the earlier interpretation that low toughness due to the absence of delamination occurs when cleavage parallel to the macroscopic fracture plane becomes the easier option.

Fig. 9 shows the estimated fraction of ferrite grains as a function of the

angle between the {100} plane normal and the rolling direction, obtained from the EBSD analysis with a tolerance angle of 11.25°. This particular value of tolerance angle corresponds to half of the tilt angle 22.5° which permits the optimum capture the ferrite grains whilst avoiding overlap among grains in the calculations [26]. The fraction is balanced about 45° to RD, because of the symmetry of {100} plane in the cubic lattice. The fractions quoted at 0°, 90° to RD and at 22.5°, 67.5° to RD, therefore come from the same grains. A hypothetical fraction of randomly oriented 10,000 grains was created in a computer simulation for comparison. The set of generated grains satisfied the distribution of misorientation angles for a randomly textured polycrystalline sample [34]. It is evident that the diagonal Charpy-test orientation is most susceptible to easy cleavage parallel to the macroscopic fracture plane.

Finally, it is appropriate to point out that considerable work was done to investigate whether the density of grain boundaries is a function of test orientation, and to study any anisotropic distribution of inclusions. Neither of these were found to be relevant [31].

4. Conclusions

The orientation-dependence of Charpy properties in two variants of hot-rolled linepipe steels has been studied.

1. The toughness is found to be particularly sensitive to the orientation of the test samples relative to the macroscopic frame of reference of the rolled plates, when the toughness is measured in the temperature regime corresponding to the ductile-brittle transition.
2. Broken Charpy samples which exhibit delamination parallel to the rolling plane are associated with a greater energy absorbed during fracture than those which do not delaminate, but fail by cleavage.
3. The toughness is reduced when the conditions necessary to promote cleavage parallel to the macroscopic fracture plane of the Charpy test become less onerous compared with that required to cause delamination.
4. Those Charpy-test orientations where the crystallographic texture is such that there is a high probability of finding {100} planes parallel to the macroscopic fracture plane, have poor toughness in the temperature regime where the material experiences a ductile-to-brittle transition.

5. It is the texture, therefore, that explains the dip in toughness experienced when the long direction of a Charpy specimen is at 45° to that of rolling.

Acknowledgements: The authors are grateful for support from the POSCO Steel Innovation Programme, and to the World Class University Programme of the National Research Foundation of Korea, Ministry of Education, Science and Technology, project number R32-2008-000-10147.

[1] D. H. Seo, C. M. Kim, J. Y. Yoo, K. B. Kang, in: Seventeenth International Offshore and Polar Engineering Conference, The International Society of Offshore and Polar Engineers, California, USA, 2007, pp. 3301–3306.

[2] D. Stalheim, K. Barnes, D. McCutcheon, in: Microalloyed Steels for the Oil and Gas Industry, TMS, Warrendale, Pennsylvania, USA, 2007, pp. 73–108.

[3] K. B. Kang, H. H. Bae, W. Y. Choo, in: R. Denys (Ed.), Proceedings of the 4th International Pipeline Technology Conference, volume 4, Scientific Surveys Ltd., Ostend, Belgium, 2004, pp. 1689–1699.

[4] K. Kim, J.-H. Bae, in: 2008 7th International Pipeline Conference, volume 3, ASME, New York, USA, 2008, pp. 167–173.

[5] C. E. Sims, Trans. Met. Soc. AIME 215 (1959) 367–393.

[6] J. M. Hodge, R. H. Frazier, F. W. Boulger, Trans. Metall. Soc. AIME 215 (1959) 745–753.

[7] T. J. Baker, J. A. Charles, Journal of the Iron and Steel Institute 210 (1972) 680–690.

[8] P. C. Wilson, Y. V. Murty, T. Z. Kattamis, R. Mehrabian, Metals Technology 2 (1975) 241–244.

[9] Y. I. Matrosov, I. E. Polyakov, Stal 2 (1976) 162–167.

[10] S. J. Garwood, in: Application of Fracture Mechanics to Materials and Structures, Martinus Nijhoff Publishers, Leiden, Holland, 1984, pp. 939–950.

[11] G. S. Kramer, G. M. Wilkowski, W. A. Maxey, Flaw tolerance of spiral–welded line pipe, Technical Report L51514, American Gas Association, Washington, D. C., USA, 1987.

[12] V. A. Burnos, T. P. Vaschilo, L. E. Balandina, Industrial Laboratory (USSR) 54 (1988) 548–550.

[13] G. M. Wilkowski, J. Ahmad, F. Brust, N. Ghadiali, P. Krishnaswamy, M. Landow, C. W. Marschall, P. Scott, P. Vieth, Short cracks in piping and piping welds, Technical Report NUREG/CR-4599-Vol.1-No.1; BMI–2173-Vol.1-No.1, Nuclear Regulatory Commission, Ohio, USA, 1991.

[14] P. Krishnaswamy, P. Scott, R. Mohan, S. Rahman, Y. H. Choi, F. Brust, T. Kilnski, N. Ghadiali, C. Marchall, G. Wilkowski, Fracture behavior of short circumferentially surface-cracked pipe, Technical Report NUREG/CR-6298, Nuclear Regulatory Commission, Ohio, U. S. A., 1995.

[15] B. Mintz, W. B. Morrison, P. I. Welch, G. J. Davies, in: G. Gottstein, K. Lucke (Eds.), Texture of Materials, volume 2, Springer–Verlag, Berlin, Germany, 1978, pp. 465–474.

[16] H. Inagaki, K. Kurihara, I. Kozasu, Trans. Iron Steel Institute of Japan 17 (1977) 75–81.

[17] G. J. Baczynski, J. J. Jonas, L. E. Collins, Metallurgical & Materials Transactions A 30 (1999) 3045–3054.

[18] R. H. Petrov, O. L. Garcia, J. J. L. Mulders, A. C. C. Reis, J. H. Bae, L. A. I. Kestens, Y. Houbaert, Materials Science Forum 550 (2007) 625–630.

[19] J. B. Ju, J. S. Lee, J. I. Jang, Materials Letters 61 (2007) 5178–5180.

[20] B. Mintz, W. B. Morrison, P. P. Morris, G. J. Davies, in: G. J. Davies (Ed.), Texture and Properties of Materials, The Metals Society, London, U.K., 1976, pp. 224–234.

[21] D. M. Fegredo, B. Faucher, M. T. Shehata, in: Strength of Metals and Alloys, volume 2, Pergamon Press, Oxford, U. K., 1985, pp. 1127–1132.

[22] O. L. Garcia, R. Petrov, J. H. Bae, L. Kestens, K. B. Kang, Advanced Materials Research 15–17 (2007) 840–845.

[23] I. Pyshmintsev, A. Gervasyev, R. H. Petrov, V. C. Olalla, L. A. I. Kestens, Materials Science Forum 702–703 (2012) 770–773.

[24] R. Petrov, O. L. Garcia, N. S. Mourino, L. Kestens, J. H. Bae, K. B. Kang, Materials Science Forum 558–559 (2007) 1429–1434.

[25] Anonymous, ASM Handbook: Irons, Steels, and High-Performance Alloys, volume 1, ASM International.

[26] M. S. Joo, D. W. Suh, J. H. Bae, H. K. D. H. Bhadeshia, Materials Science & Engineering A 546 (2012) 314–322.

[27] M. S. Joo, D.-W. Suh, J. H. Bae, N. S. M. no, R. Petrov, L. A. I. Kestens, H. K. D. H. Bhadeshia, Materials Science & Engineering A 556 (2012) 601–606.

[28] A. F. Gourgues, H. M. Flower, T. C. Lindley, Materials Science and Technology 16 (2000) 26–40.

[29] M.-C. Kim, Y. J. Oh, J. H. Hong, Scripta Materialia 43 (2000) 205–211.

[30] D. Bhattacharjee, J. F. Knott, C. L. Davis, Metallurgical & Materials Transactions A 35 (2004) 121–130.

[31] M. S. Joo, Anisotropy of Charpy Properties in Linepipe Steels, Ph.D. thesis, Pohang University of Science and Technology, Pohang, Republic of Korea, 2012.

[32] T. Tanaka, International Metals Reviews 4 (1981) 185–212.

[33] R. Ayres, D. F. Stein, Acta Metallurgica 19 (1971) 789–794.

[34] J. K. Mackenzie, Biometrika 45 (1958) 229–240.

Table 1: Chemical composition (wt%) and thermomechanical processing conditions. Ar_3 represents the temperature at which austenite begins to decompose during cooling. Please note that the exact chemical composition and processing is proprietary information.

Steel	C	Mn	Si	P+S	Nb+Ni+Mo	Ti+Al	V+Cr+Cu	N
$X80_{REF}$ [26]	< 0.08	< 2.0	0.21	< 0.013	< 0.8	0.03	-	< 0.0036
$X80$	< 0.06	< 2.0	0.31	-	< 0.5	0.02	0.30	-
$X70$	< 0.08	< 1.7	0.25	-	< 0.4	0.03	0.15	-

Reheating temperature	1100–1180°C
Cooling start–temperature	Above Ar_3
Finish rolling temperature	Above Ar_3
Coiling temperature	> 500°C

Table 2: Fractions of phases in the steels.

Steel	Allotriomorphic ferrite	Bainitic ferrite	Others
$X80_{REF}$ [26]	0.17±0.02	0.83±0.02	MA, Pearlite
$X80$	0.14±0.01	0.86±0.01	MA
$X70$	0.29±0.07	0.71±0.07	MA, Pearlite

Table 3: Grain sizes of the steels in μm. Crystallographic grain sizes defined by for two different assumptions regarding misorientation, $\geq 2°$ and $15°$ respectively.

Steel	Misorientation $\geq 2°$	Misorientation $\geq 15°$
$X80_{REF}$ [26]	1.5±1.5	10.3±3.8
$X80$	1.4±1.5	11.3±4.2
$X70$	1.6±1.5	9.1±3.0

Table 4: Tensile test data representing mean values of three tests done at each orientation. The data for $X80_{REF}$ are from [26].

Steel	Orientation	Yield strength MPa	Ultimate strength MPa	Total elongation %	Uniform elongation %
$X80_{REF}$	transverse	634±29	707±16	14.7±1.1	7.1±1.4
	diagonal	600±35	663±10	15.8±1.9	7.7±1.9
	longitudinal	602±35	676±4	13.0±2.0	7.1±1.7
$X80$	transverse	633±8	722±4	15.8±0.7	8.6±0.3
	diagonal	582±13	667±6	19.7±0.7	10.2±0.3
	longitudinal	572±9	691±3	17.1±0.9	10.1±0.3
$X70$	transverse	581±2	657±5	17.1±1.5	9.5±0.4
	diagonal	528±2	608±3	21.6±0.5	10.4±0.3
	longitudinal	528±17	631±5	15.4±1.2	9.9±0.2

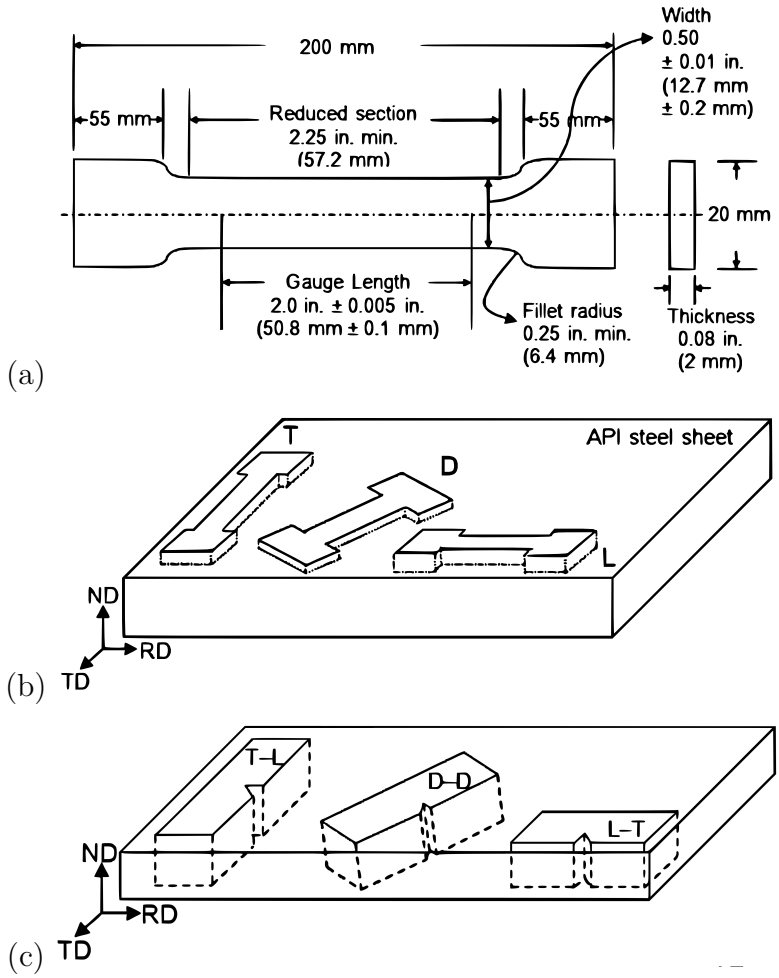

Figure 1: Orientations of test samples relative to steel plate. 'RD', 'TD' and 'ND' represent rolling, transverse and normal directions. (a) Tensile test sample. (b) Orientations of tensile test samples. 'T', 'D' and 'L' stand for transverse, diagonal and longitudinal respectively. (c) Orientations of Charpy specimens with 'L–T', 'T–L' and 'D–D' designations, in which the first letter represents the sample direction and the second the impact direction.

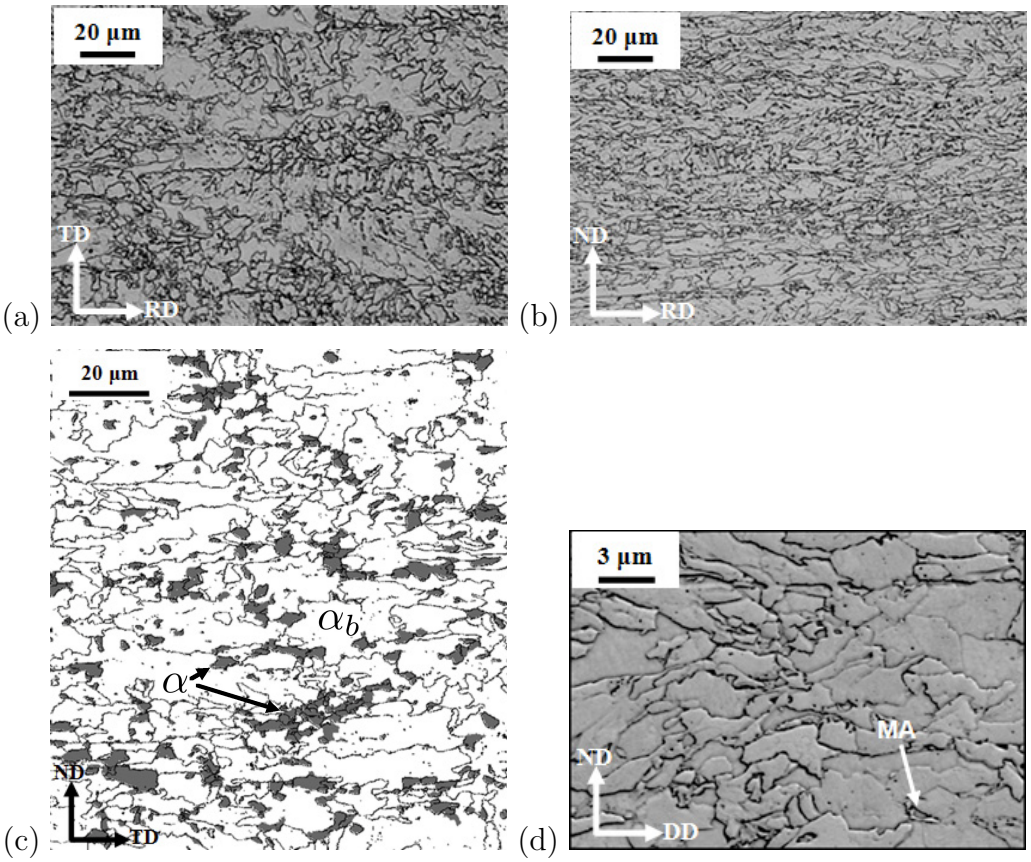

Figure 2: Microstructure of $X80$. (a) Optical micrograph of section parallel to rolling plane, and (b) normal to the rolling plane. (c) Map showing the spread in crystallographic orientation; boundaries are identified by misorientations $> 15°$, and the dark areas are allotriomorphic ferrite in which the grains have internal misorientations $< 1.5°$, whereas the white regions contain much greater internal-misorientations and are bainitic. (d) Scanning electron micrographs of surface normal to the DD direction.

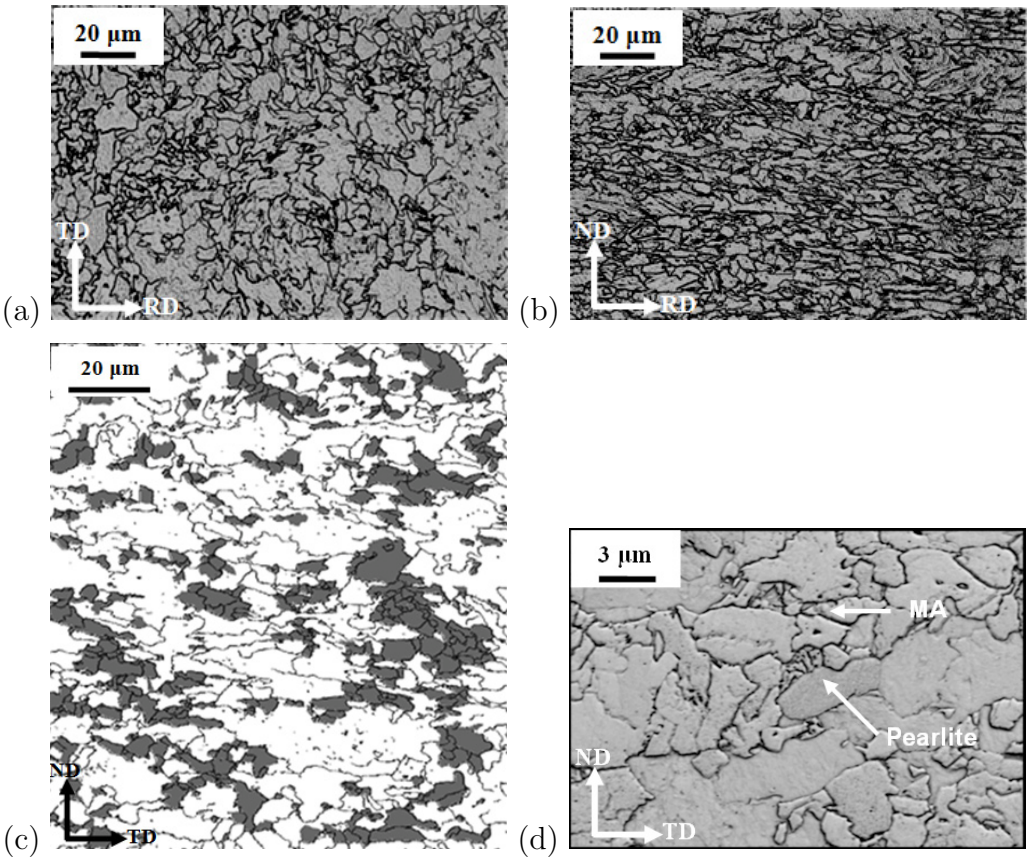

Figure 3: Microstructure of $X70$. (a) Optical micrograph of section parallel to rolling plane, and (b) normal to the rolling plane. (c) Map showing the spread in crystallographic orientation; boundaries are identified by misorientations $> 15°$, (d) scanning electron micrograph of surface normal to rolling direction.

(a) 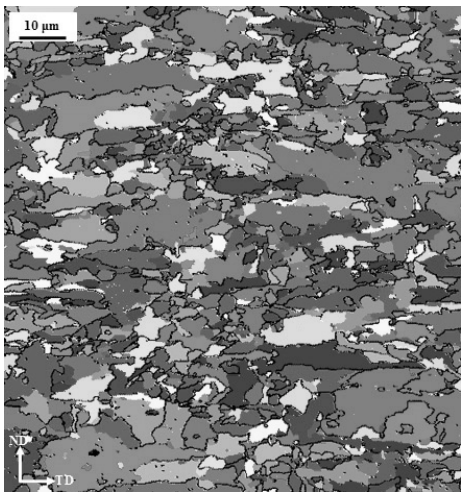

(b) 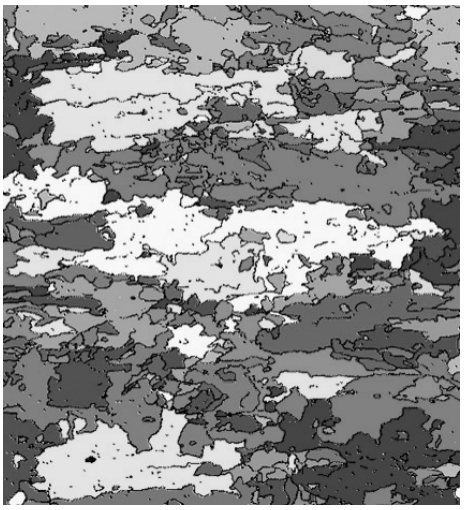

Figure 4: Grain maps of surface normal to RD in $X80$ steel. The maps represent the difference in grain size between when grain boundary misorientation is greater than (a) 2° and (b) 15°. Black lines represent grain boundaries and each grain is highlighted in its own colour.

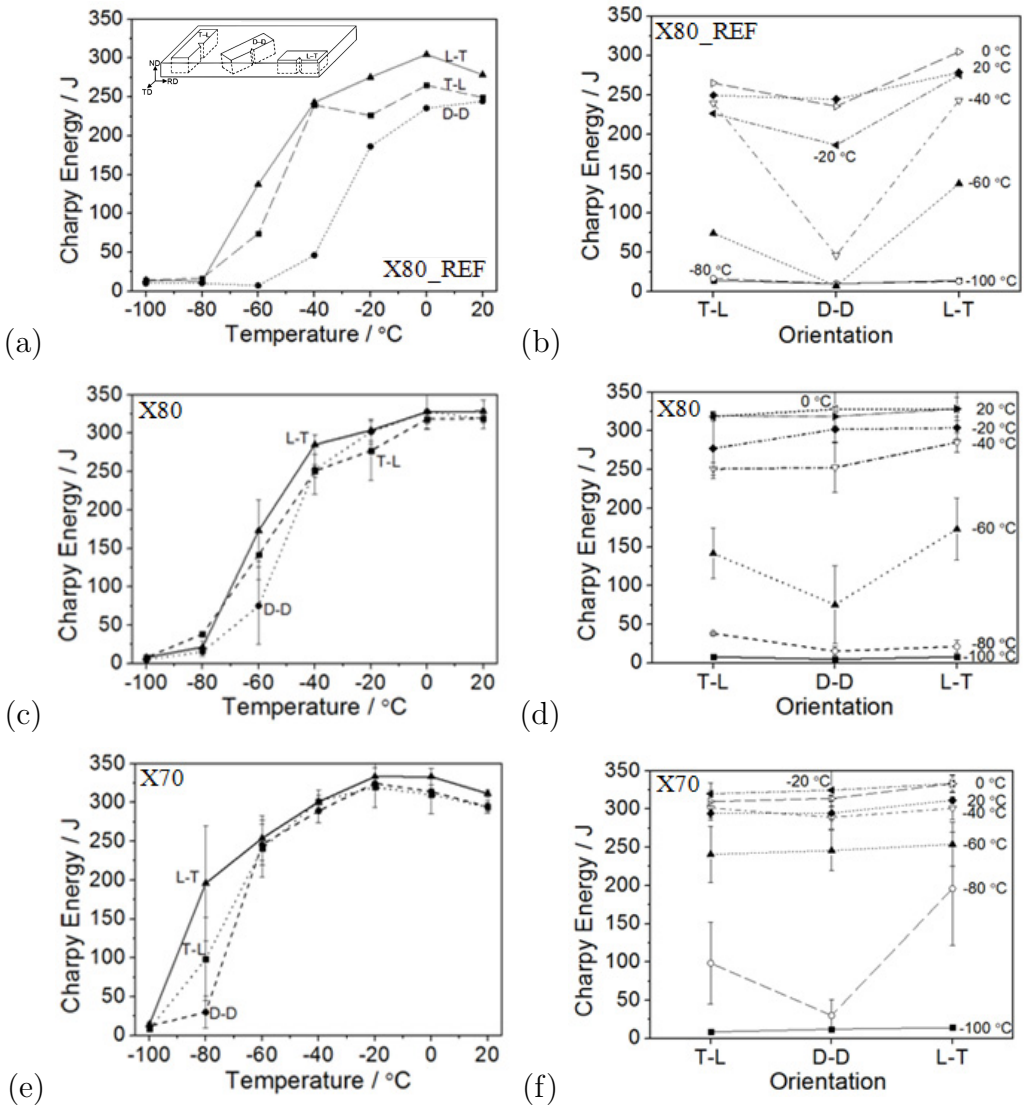

Figure 5: Charpy impact test results as a function of temperature of (a) $X80_{REF}$ [26], (c) $X80$ and (e) $X70$, and as a function of orientation of (b) $X80_{REF}$, (d) $X80$ and (f) $X70$.

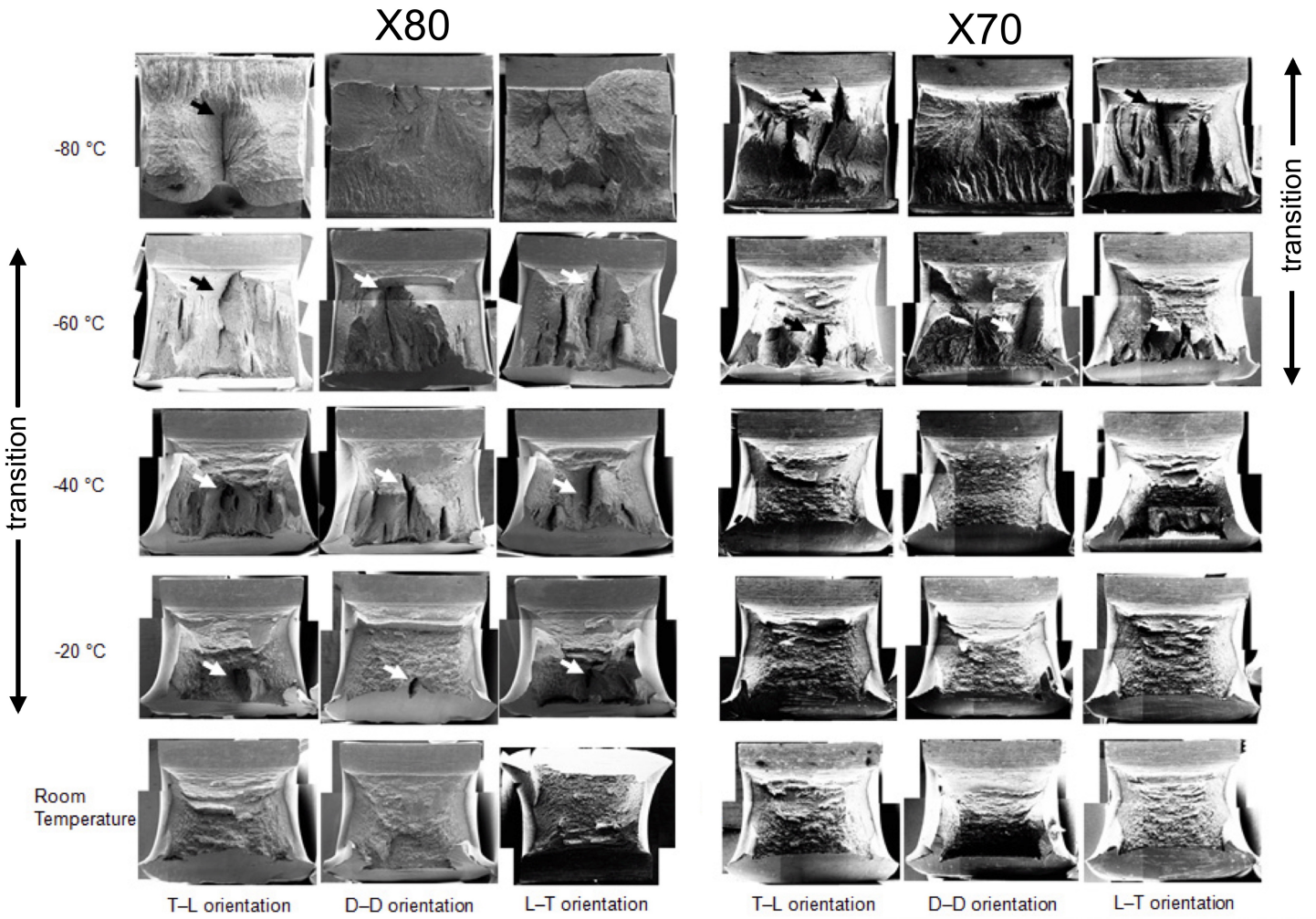

Figure 6: Broken X80 and X70 steel Charpy specimens with delamination indicated by black and white arrows.

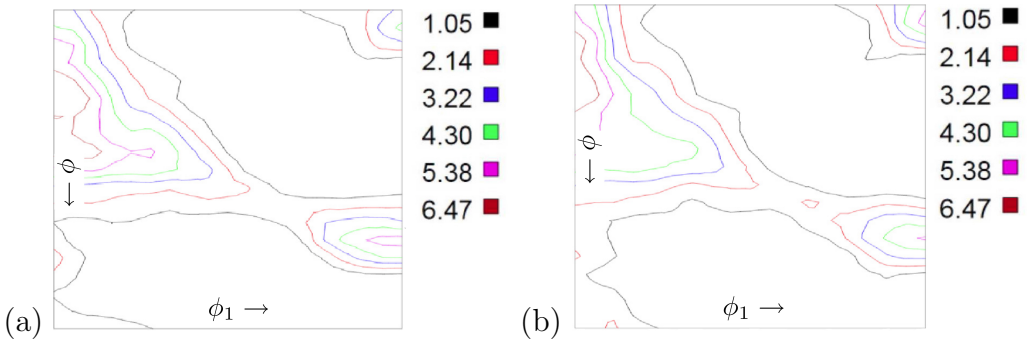

Figure 7: Sections of the orientation distribution function at $\phi_2 = 45°$ with ϕ, ϕ_1 ranging from 0 to 90°. (a) $X80$ and (b) $X70$.

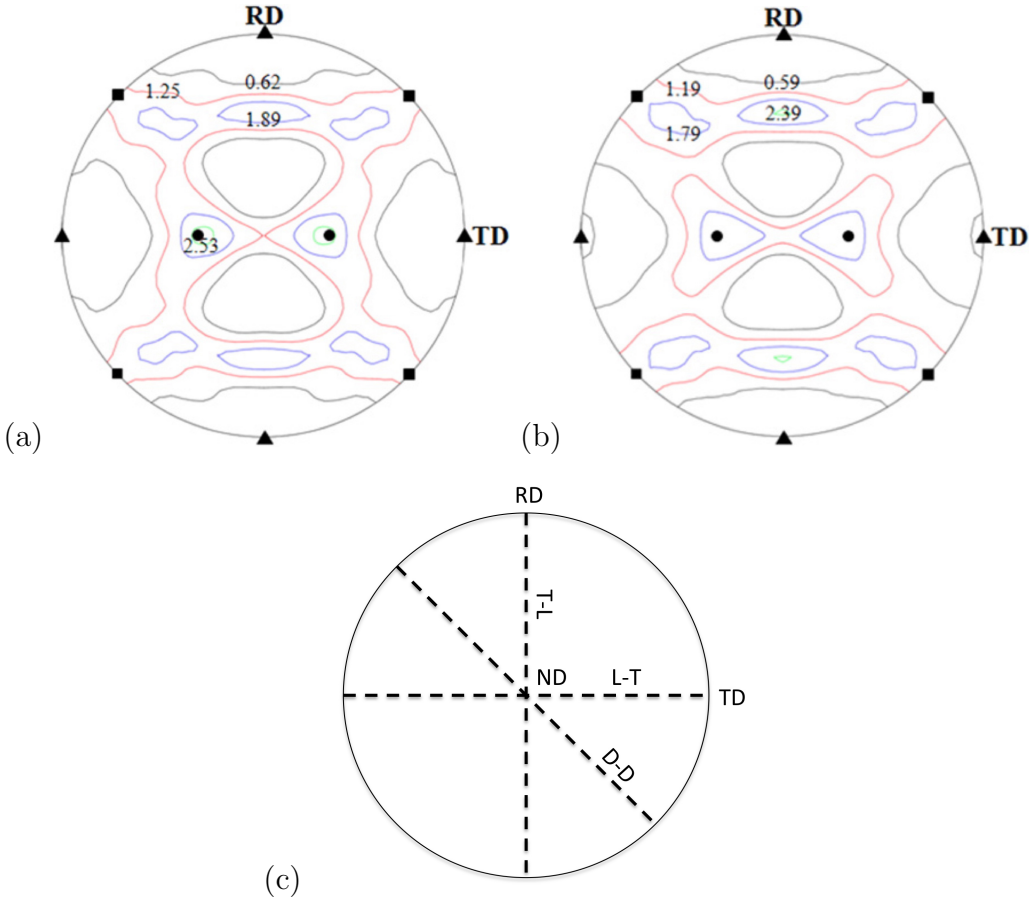

Figure 8: {200} pole figures showing significant texture components: ●{112}⟨110⟩, ■{001}⟨110⟩ and ▲{001}⟨100⟩. (a) $X80$; (b) $X70$; (c) dashed lines showing the traces of the macroscopic fracture plane of each Charpy test sample orientation.

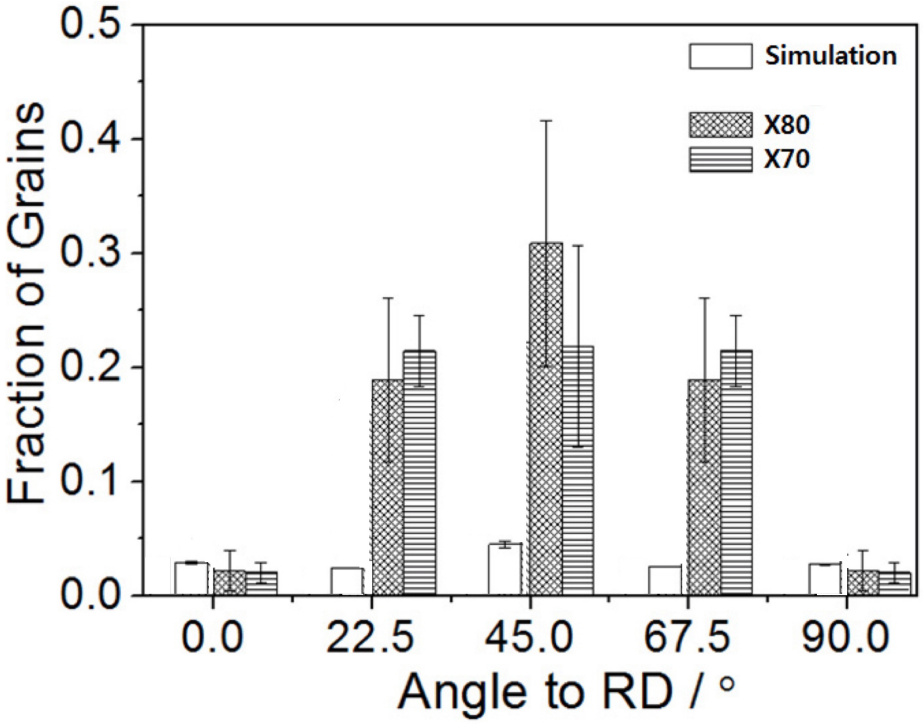

Figure 9: Fraction of grains for which the {100} plane normal is within the tolerance angle of 11.25° have a {100} plane parallel to the macroscopic fracture-surface, as a function of angle between the normal to the {100} planes and the rolling direction. Note that the sum of the fractions will not equal 1 because not all grains have {100} parallel to the fracture surface within the tolerance angle.